Eurographics Workshop on Visual Computing for Biology and Medicine (2018)
A. Puig Puig, T. Schultz, and A. Vilanova (Editors)

VisualFlatter Visual Analysis of Distortions in the Projection of Biomedical Structures

Nicolas Grossmann[1†], Thomas Köppel[1†], M.Eduard Gröller[1,2], Renata G. Raidou[1]
[1]TU Wien, Austria, [2]VRVis Research Center, Austria

Abstract

Projections of complex anatomical or biological structures from 3D to 2D are often used by visualization and domain experts to facilitate inspection and understanding. Representing complex structures, such as organs or molecules, in a simpler 2D way often requires less interaction, while enabling comparability. However, the most commonly employed projection methods introduce size or shape distortions, in the resulting 2D representations. While simple projections display known distortion patterns, more complex projection algorithms are not easily predictable. We propose the VisualFlatter, a visual analysis tool that enables visualization and domain experts to explore and analyze projection-induced distortions, in a structured way. Our tool provides a way to identify projected regions with semantically relevant distortions and allows users to comparatively analyze distortion outcomes, either from alternative projection methods or due to different setups through the projection pipeline. The user is given the ability to improve the initial projection configuration, after comparing different setups. We demonstrate the functionality of our tool using four scenarios of 3D to 2D projections, conducted with the help of domain or visualization experts working on different application fields. We also performed a wider evaluation with 13 participants, familiar with projections, to assess the usability and functionality of the Visual Flatter.

CCS Concepts

•Human-centered computing → Visual analytics; •Applied computing → Life and medical sciences;

1. Introduction

Projections are often used in the field of visualization, as they simplify complex structures by mapping them to 2D representations. This is particularly important in medical visualization [KMM*18], as they allow visualization and domain experts to inspect the data with possibly fewer interactions. They also enable users to understand the morphology of the data and facilitate comparative tasks.

Projections are often created through a mapping procedure (flattening), where each position from the original 3D spatial domain is assigned to a new position in the target 2D spatial domain. Commonly, this process introduces distortions in the initial 3D structure, which leads to changes in its size or shape. In case of simple projections, such as the ones employed in cartography [Sny97], the introduced distortions are often known and expected. However, for more complex algorithms [VW08], the perception of distortions becomes more difficult. Knowing the sources of projection-related distortions can lead to improved visualization results, and to a better understanding of the general capabilities of projection methods.

In this work, we employ as *proof-of-concept* a commonly employed unwarping algorithm, which transforms 3D meshes into 2D cartographic projections, in two steps. First, the input mesh of the structure is inflated to a sphere. Then, this sphere is unfolded onto a 2D plane, using one of several alternative map-inspired projection methods and a pre-defined cutting plane. For the mapping, different possibilities can be selected [Sny97], which might preserve or distort different parts of the structures. Defining an appropriate cutting plane can also have a significant impact on the final outcome.

As mentioned before, the impact of these alternatives is not known a-priori, and an informed choice based on the potentially introduced distortions is required. Traditionally, distortions are shown employing checkerboard patterns. Yet, checkerboards do not allow understanding how and at which specific step of the process these distortions have been introduced. Also, comparability across the steps can be tedious and time-consuming with checkerboards.

To provide experts working on projection algorithms with a better understanding of the introduced distortions, we designed and implemented a visual exploration tool, the *VisualFlatter*. Our tool is meant to enable visualization and domain experts to explore and analyze distortions in the resulting projections, with sufficient de-

† *Both authors contributed equally to this work.*

DOI: 10.2312/vcbm.20181242

tail. Additionally, it allows them to form and/or confirm hypotheses, with respect to the generation of the resulting distortions.

The contribution of our work is the design and implementation of a visual tool, the *VisualFlatter*, which supports users working with projection-based visualizations of 3D structures to perform the following tasks:

- **(T1)** – Exploration and analysis of the distortions introduced by a projection method on the final projected representation.
- **(T2)** – Exploration and analysis of the progression of distortions over the projection pipeline (e.g., inflation and unfolding).
- **(T3)** – Exploration and informed selection of appropriate projection parameterizations.

The above-described capabilities of the *VisualFlatter* can be applied on the whole mesh, or on manually selected sub-regions of the input mesh. To the best of our knowledge, an interactive tool that enables the exploration, analysis and informed decision making with respect to distortions in projected representations of biomedical structures has not been proposed before.

2. Background: Projections

Many applications of medical visualization employ projections from 3D structures to 2D map-like representations. Some examples include projections for the analysis of the circulatory system, the colon, tumors and the brain [KMM*18]. Many of these techniques involve the projection (or flattening) of structures into 2D planar representations, using methods from the field of mesh parameterization. These projection techniques are popular in medical visualization, because of their ability to display complex 3D structures, in an easy and understandable 2D manner. Furthermore, 2D representations require possibly less interaction and enable users to complete exploratory tasks, such as diagnosis or comparison, in a cognitively less demanding way.

There is a large variety of projection methods in (biomedical) visualization literature, which we review in the upcoming section. Within this work we focus, as proof-of-concept, on projection techniques, which require inflating a 3D structure to a sphere and then, unfolding it onto a 2D plane. An example of such method has been used in the work of Krone et al. [KFS*17]. Although such methods are simple and commonly employed in visualization applications, they are often accompanied by distortions [KMM*18], and there is a large variety of methods for the inflation, flattening and cutting of the input 3D structure – often, a triangulated mesh.

Several different approaches have been used in the past for the inflation of meshes to spheres [KFS*17, PS09, PH03, RS07, HK14]. For the unfolding and flattening of the resulting sphere to a 2D map, often cartographic inspired projection methods [Sny97] are employed. Commonly used projection types are able to prioritize the preservation of the area (equiareal) or the angle (conformal) of the input meshes. Depending on the case, different projections methods are considered more appropriate. For example, conformal mapping is often used for the unfolding of the colon, during virtual colonoscopy [HATK00]. The reason for that is that curvature is an important indicator for possible polyps. Therefore, the angle should not be distorted during the unfolding to reliably use the 2D maps for polyp examination. On the other hand, equiareal mappings are used if the preservation of the size of the structures is crucial for diagnosis or decision making of an appropriate treatment. An example of such a mapping can be used during risk assessment of tumor treatment with radiotherapy [RCMA*18].

Although projections have been vastly researched and employed in medical visualization, the exploration and analysis of the distortions introduced in the resulting representations **(T1)** have not been equally investigated. Yet, studying the generation process of these distortions **(T2)** and being able to conduct informed choices **(T3)**, when designing a method for the projection of a 3D structure to a 2D plane, is of high importance for visualization experts and the domain experts, who will be using the resulting representations.

3. Related work

The *VisualFlatter* aims at facilitating the visual analysis of distortions during the generation of mesh projections on 2D planes. With the exception of the work of Saroul et al. [Sar06], who investigated the distortions introduced by different projection methods, there is no previous work in the exact direction of the visual analysis of such distortions. In this section, we review related work, which either employs projection-based methods in the proposed visualizations, or focuses on the visual analysis of errors or distortions.

Projection-Based Visualizations. There is vast work on projection-based visualizations for several applications. A few examples include vessel visualizations [AH11, AMB*13, KFW*02, Mis13], colon unfoldings [HATK00, VBWKG01], visualizations of bones [KBH*10, KST*14, KLR*13] and of other organs, such as the myocardium [TBB*08], the placenta [MMK*17] or the bladder [RCMA*18]. All projection-based visualization work has been recently summarized and classified in a state-of-the-art report by Kreiser et al. [KMM*18]. We hereby review the most relevant approaches – some of which, will be employed also as usage scenarios in Section 5.1.

Krone et al. [KFS*17], Balasubramanian et al. [BPS10], Khosravi et al. [KSZ14] and Zhu et al. [ZHT05] proposed methods of projecting 3D structures onto 2D maps. However, in all these cases, the main focus is not on evaluating the distortions introduced by the projection. Krone et al. [KFS*17] presented a method of flattening molecules to visualize them on a 2D map, where the molecules are inflated to a sphere and, subsequently, map projections are applied to represent the whole molecule onto a 2D surface. For quality assessment, they color encode and analyze the error – by means of traveled distance by each vertex. Balasubramanian et al. [BPS10] developed a near-isometric technique of representing the brain in 2D and show the color-coded, per-vertex error in 3D and 2D. Khosravi et al. [KSZ14] presented a way of representing the cortical volume by using a set of partial iso-surfaces which improves the flattening performance. They show distortions – in area or angle – globally by a variance plot. Zhu et al. [ZHT05] developed a conformal mapping of blood vessels followed by an area preserving optimization and underline the effectiveness of their tool by histograms that show the area change ratio.

In all these cases, the authors do not employ any interactive

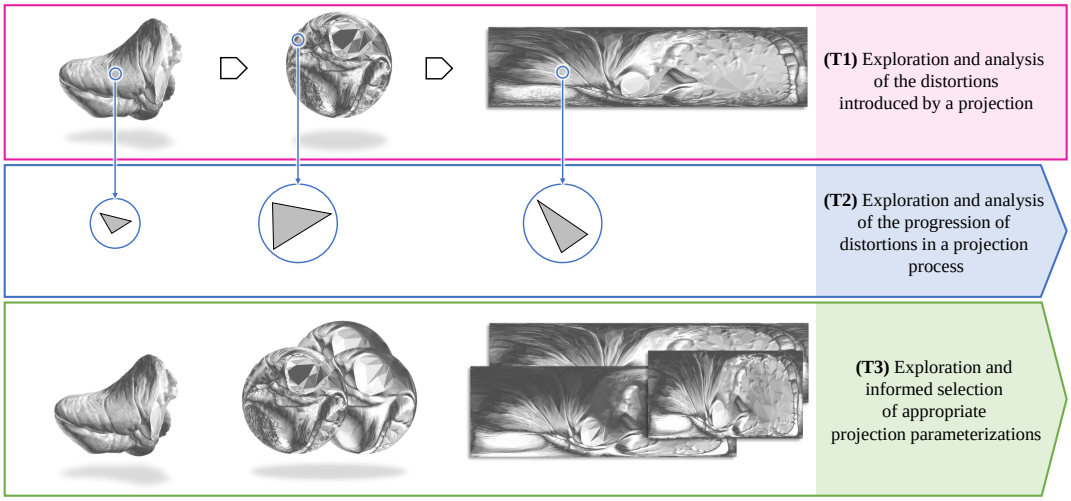

Figure 1: *Workflow of the VisualFlatter, with its proposed main components **(T1-T3)**.*

methods for the exploration and analysis. Also, they do not focus on how this error was generated or on how it could be possibly minimized. The *VisualFlatter* allows the detailed investigation of the distortion that is introduced during the projection steps both globally and locally, while it also allows a follow-up of the evolution of these errors through the projection procedure.

Visual Analysis of Mesh Errors. In the field of visual analysis of errors, the visualizations proposed by Reiter et al. [RBGR18], Raidou et al. [RMB*16], Silva et al. [SMS09] and Schmidt et al. [SPA*14] allow a comparison of meshes and an analysis of errors, introduced during the generation or deformation of meshes.

Reiter et al. [RBGR18] recently presented a web-based framework to facilitate the exploration and detailed analysis of shape variability, allowing segmentation experts to generate hypotheses, in relation to the performance of the involved algorithms and the respective segmentation errors. Before this, Raidou et al. [RMB*16] had proposed a visual analytics tool allowing an investigation of errors that occur when automatically segmenting organs to improve segmentation algorithms. A triangle-to-triangle correspondence between meshes allows to compute the mean and standard deviation of errors on each triangle. The errors are visualized in a scatterplot matrix that allows brushing and is linked to the 3D view of the respective organs. Different quality measures can be visualized on the mesh by color coding. Silva et al. [SMS09] developed a tool called PolyMeCo to analyze and compare meshes. They allow the comparison of meshes with respect to a reference mesh by color coding the differences, i.e., the mean curvature, and the comparison of several meshes by histograms. Schmidt et al. [SPA*14] focus on the comparative visual analysis of 3D meshes, reconstructed from point clouds. The reconstruction error is shown by color encoding on the mesh. Regions of high error can be analyzed and compared in a parallel coordinates plot view, to other reconstruction algorithms. A magic lens tool allows a selection of an arbitrary region to analyze the distortions.

In contrast to previous work, our approach allows the investigation of errors that have been generated across several steps of the projection procedure. In addition to that, the *VisualFlatter* enables decision making with respect to parameterizations of the projection procedure, i.e., it allows the users to select a setup and interactively perform a projection, which will induce less distortions in the outcome 2D representation. These two tasks can be performed on the entire mesh and on user-defined sub-regions.

4. The design of the *VisualFlatter*

The *VisualFlatter* was designed and implemented, as a means for the visual analysis of distortions introduced during the projection of 3D meshes onto 2D maps. It aims at the exploration of the progression of the distortions over the projection pipeline and at providing aid for decision making when selecting a specific projection setup. The tasks that can be accomplished with the use of our proposed tool are schematically depicted in Figure 1.

4.1. Exploration and analysis of projection distortions (T1)

A proof-of-concept projection used within the *VisualFlatter* is similar to projecting the earth onto a map. To be able to apply this approach on arbitrary 3D organ meshes, we need to first project them onto a sphere, using the algorithm by Choi et al. [CLL15]. Then, we map the sphere to the 2D domain [Sny97]. The sphere transformation step provides the option to generate an angle- or an area-preserving mapping, with the latter being an iterative approach that minimizes the distortions. We modified the basic inflation algorithm in two ways: first, by making the resulting sphere rotation match more closely the original mesh; second, by finding a different initial vertex placement that increases the speed of convergence of the iterative version in some cases. As the last step in our projection, we unfolded the created sphere in such a way that we make a cut at the backside of the sphere – as defined by the camera position, and then apply a cartographic projection to unfold it into 2D.

As mentioned in Section 2, there are different projection methods, mostly inspired by the field of cartography. Among these, the

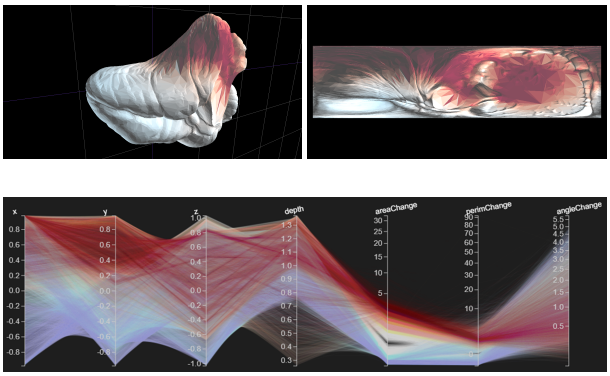

Figure 2: *Global analysis of a projection, using the unfolding of the cerebellum. Our example shows the 3D mesh of the cerebellum (top left), its 2D projection (top left) and the PCPs for the exploration of the distortion measures (bottom), color-coded by area distortion.*

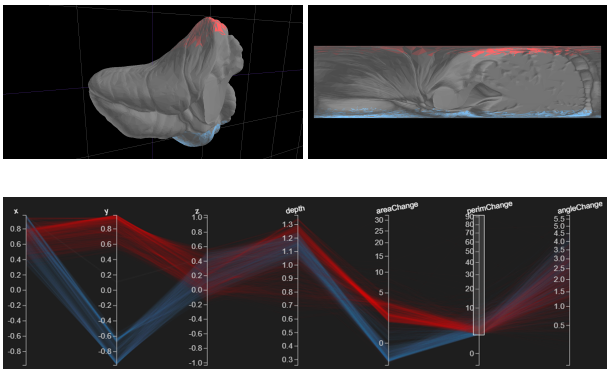

Figure 3: *An example of region-based analysis of distortions in a cerebellum unfolding. Two regions have been selected (red and blue), by brushing along the axes of the PCP (distortion-based selection). The triangles of the 3D and 2D views, and the PCP polylines are colored distinctly for the two regions.*

Mercator projection is very well-known [Sny97]. It is a conformal mapping that preserves the angles, but not the area, of the input 3D mesh. Other known projections include the Lambert projection [Sny97], which is an area-preserving technique. In both cases, the regions around the poles are more distorted. Within our tool, we enable the users to perform interactively both the Mercator and Lambert projections. However, the tool can be extended to use different mapping techniques [CPS13, FH05, NSZ*17], and also other projection techniques that not necessarily require the step of inflating the mesh to a sphere. For the cutting plane, the three anatomical planes, or a manually, arbitrarily selected plane can be selected.

In order to explore and analyze the distortions, we assume a bijective triangle-to-triangle correspondence between the initial 3D domain and the resulting 2D mapping. We used the change in the *area*, *angle* or *perimeter* of the triangles of the structure, as measures for the distortion [FH05]. Additional features, such as shape or shortest distance preservation, could also be incorporated as distortion measures, depending on which are preserved or distorted.

Global analysis of distortions. The first step when inspecting the results of a projection technique is to compare the 3D input with the 2D transformed output, at a global level. The user must be able to judge the overall behavior of the projection and to get a quick overview of how the projection affects a mesh, as a whole. To this end, the interface of the *VisualFlatter* starts by displaying the 3D mesh and the 2D projected representation, side-by-side. We quantify the distortion introduced by the projections, in terms of the previously discussed triangle area, perimeter and angle differences between the two representations. These distortion measures are color encoded directly on the triangular mesh and the 2D projected map, as shown in Figure 2. We employ different colormaps depending on the visualized distortion measure, i.e., a diverging colormap is employed for values revolving up and below zero, following guidelines from ColorBrewer [HB03]. The user can select which distortion measure to inspect and the colormap can be interchanged, on demand. With this simple, yet effective, linking through color encoding, the user can mentally associate regions from the two representations, identify where certain parts were moved during the transformation and determine regions of particular interest with respect to the introduced distortions.

The 3D and 2D views provide a quick overview of the projection outcome. Still, certain correlations between the employed distortion measures and the underlying geometric features that might have led to them (e.g., sphere mapping algorithms heavily distorting points close to the center) are not straightforward to inspect. To support a more detailed exploration of the distortion measures with respect to the anatomic/geometric features of the projected structures, we used a *Parallel Coordinates Plot* (PCP) [Ins85], as shown in Figure 2. PCPs were preferred over other multi-dimensional representations, such as scatterplot matrices, for their versatility in depicting correlations and patterns across the represented variables. In our PCP, one polyline corresponds to one triangle in the 3D mesh and the axes correspond to the calculated distortion measures of the triangle (area, perimeter, angle), geometric properties such as their position and the distance to the center (depth). The PCP view can be enriched with some custom per-triangle properties provided for certain datasets, as we will show later in the paper. The polylines are also colored based on the value of a certain distortion measure, as selected also for the 3D and 2D views. Standard density plotting, filtering, and brushing and linking (to the 3D and 2D views) are employed to increase the visibility of polylines and patterns, as well as to enable correspondence between the different views. Given the high number of triangles, we use a progressive rendering of the polylines, where the data is processed and rendered in a queue, avoiding to wait for the rendering to finalize.

Region-based analysis of distortions. Inspecting the input mesh and its 2D projected map as a whole provides an overview and allows the assessement of the overall performance of a specific projection algorithm. However, such analysis may obfuscate important details of the projection process. To enable a local analysis of different parts of the initial mesh, we follow a straightforward approach, where the user can manually split the mesh into sub-regions, i.e., groups of neighboring triangles.

Possible ways of creating these regions would either be to select and divide them based on their *distortion characteristics* (e.g.,

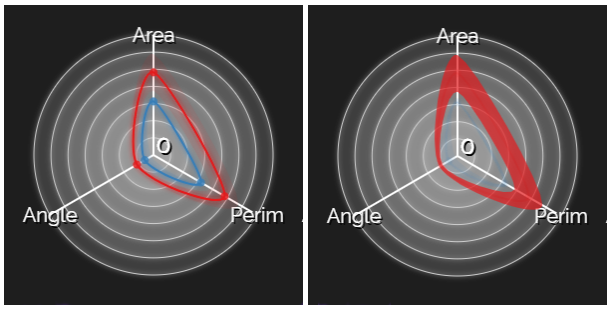

Figure 4: *A radar plot depicting the three distortion measures (angle, perimeter and area) for the two selected regions of Figure 3. On the left, the red and blue lines show the mean values of distortion measures of the respective regions. On the right, the area shows the range of values for the red region, when hovering over it.*

selection of parts with high angular distortion) or based on *anatomical or geometrical characteristics* (e.g., selection of the anterior lobe of the cerebellum). We offer both functionalities: the geometry/anatomy-based selection is supported by drawing with the mouse over the mesh or the 2D map directly, and the distortion-based selection is conducted using the already discussed interaction of brushing and linking along the axes in the PCP. Brushing and linking across the views enables the association of the selected regions, while each region is assigned with a different color from a qualitative coloring scheme [HB03] across all views. An example of this analysis case is depicted in Figure 3.

When performing a region-based analysis of distortions, comparison of the selected regions is required. To facilitate users to compare the distortions in each of the selected regions, we employ an additional *radar plot* [CCKT83]. Radar plots were selected as being a compact iconography representation, which combines the strengths of PCPs with glyphs. Taking advantage of the human perceptual ability to easily compare shapes, radar plots enable easy detection of patterns among different plots [Kei02] – easier than with PCPs. They are particularly suitable for our case, where a small number of variables is used. In our radar plots, the axes correspond to one distortion measure (angle, area, perimeter of triangles) and each polyline connects the mean values of each distortion measure for one selected region. Hovering on a polyline will reveal also the entire range of distortion values for each region, in the form of an area, to provide a qualitative indicator of the uniformity of a region. The colors are used consistently with the rest of the views to denote each region. An example of this is shown in Figure 4.

4.2. Exploration and analysis of the progression of distortions during the projection process (T2)

Both steps of our adopted projection approach – the inflation to a sphere and the mapping to a 2D plane – introduce distortions in the final representation of the triangles. Instead of determining the final extent of distortion in the outcome of the projection process, it would also be interesting to investigate the distortion that each one of the two previously mentioned steps introduces, individually. In practice, we want to provide functionality to answer the question: *"Which step of the process produces how much and what kind of distortion?"*. This is also relevant for other projection algorithms where several steps are followed. Comparing only the original mesh and the resulting 2D map might not be sufficient. The user should be able to interchange the displayed projection step, along with the accompanying distortions. In this way, flaws or weaknesses in the projection process can be identified and, potentially, improved later on. In this case, the representations discussed in Section 4.1 are adapted to reflect the distortions of one user-selected step through the projection process.

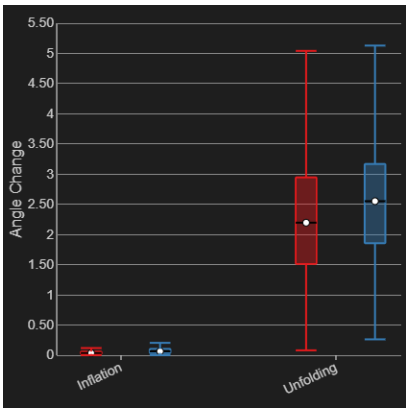

Figure 5: *A box plot showing the angle distortion that is introduced during the inflation and the unfolding steps of the projection process. This is an example of the cerebellum analysis of Figure 3. Most of the distortions are introduced during the unfolding step.*

To additionally understand the resulting distortions, it is essential to inspect the individual steps of the projection process. In this way, the users can find out which components of the projection algorithm need to be adapted to improve the results. To achieve this, we calculated the distortion also for steps in between the projection process (inflation and unfolding). Given the triangle-to-triangle correspondence through all steps, we can analyze the progression of the distortions at each step. For this, we employ a box plot representation, to aggregate the statistical attributes of the regional distortions at each step. Depicting the distortions from the individual steps side-by-side facilitates the comparison and the detection of drastic changes in the distortions, as depicted in Figure 5. As an alternative, violin plots [HN98] can also be employed.

4.3. Exploration and selection of projection setups (T3)

In the previous steps, the main goal of the *VisualFlatter* was a structured exploration and analysis workflow. In addition to this, we need to support visualization and domain users in selectively improving their projection results. Often, the resulting projections distort certain parts of the object that should not be altered in any way. Also, different setups can be followed during the projection, such as the selection of a mapping technique (e.g., Lambert or Mercator) or the cutting plane choice. In these cases, the user might try to make some educated guesses or iteratively change the projection parameters to optimize for the desired result. Instead of a trial-and-error approach, we can aid the user to perform an educated selection of the appropriate parameterization or setup for the design of the individual steps of the projection process.

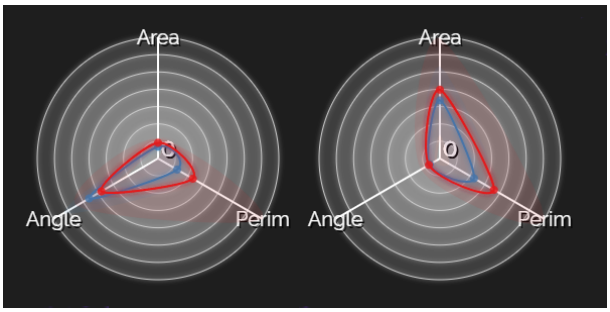

Figure 6: *Two radar plots showing the effects of the Mercator projection (on the right) and the Lambert projection (on the left) on the final distortion of the structure. The Mercator projection leads to less angular distortion, but more in area and perimeter. The Lambert projection has the opposite effect.*

To enable the comparison and selection of the most adequate configuration, we employ the previously described radar plots, juxtaposed for each configuration. By showing the different alternatives next to each other, the user can directly compare them and see the effects of configuration changes. This can be done for the whole mesh, or for selected regions, as resulting from the region splitting **(T2)**. The latter is particularly useful when highlighting semantically relevant structures, which – for example – need to be preserved, and when trying to find a specific configuration where the distortion is minimized for them, as shown in Figure 6.

Because the number of possible parameter combinations can grow quickly, we decided to only show the effects of one changing parameter, while leaving the others constant. In doing so, the user has to make iterative selections from within the given parameter space, but the effects of these choices can be monitored interactively. The user is also enabled to select among different mapping alternatives (e.g., Lambert or Mercator), as well as the desired cutting plane. The latter is performed either with predetermined planes (axial, sagittal or coronal) or with an interactive widget that allows the selection of an arbitrary plane, as depicted in Figure 7.

4.4. Implementation

The tool was implemented as a web-based application using JavaScript. More specifically, we employ Three.js for the 3D mesh view and 2D map view, and D3.js for the remaining visual representations. The mesh data is provided by a C++ server. The inflation of a mesh to a sphere is done in MATLAB using the algorithm of Choi et al. [CLL15].

5. Results

To demonstrate the general applicability of the *VisualFlatter*, we decided to perform an informal evaluation with several visualization and domain experts, who have employed projections in their work on different application fields, e.g., organ projections, or molecular maps. Each of these informal evaluations revolves around a specific usage scenario, which is presented in the following section. After the presentation and live conduction of each usage scenario, the respective interviewed expert provided us with

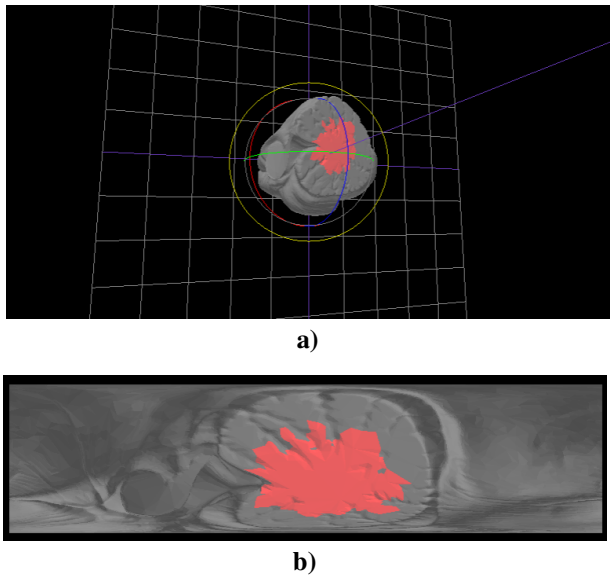

Figure 7: *The rotation controls (a) allow the user to interactively select an arbitrary cutting for the unfolding. This can be used to preserve structures of importance by placing them in the center of the map (b) and not splitting them up on the sides.*

feedback on the functionality and usability of our tool. In addition to these informal interviews, we also conducted an online evaluation with a wider public using a generic mesh. This abstraction intends to compensate for the limited number of experts available, but we took particular care that the evaluators were knowledgeable about visualization and mesh projections.

5.1. Usage scenarios and interviews with experts

For the usage scenarios conducted during the interviews with the experts from the visualization community or from the domain of the respective application, we chose four cases. In the first, a cerebellum mesh is unfolded for better presentation and diagnosis purposes [MMK*17]. The second case involves the projection of bladder radiation maps, used in risk assessment during radiotherapy treatment [PBC*16]. The third example is taken from the field of molecular visualization for the evaluation of the surface maps [KFS*17]. The last one is a more general case, where the *VisualFlatter* is used to explore, analyze and compare segmentation errors [RMB*16]. All scenarios, except for the second, have been conducted with visualization experts. This was performed with a medical physicist, who is working on the projected radiation maps.

Scenario 1: Unfolding organ meshes. In the first usage scenario and interview, a cerebellum mesh is unfolded for better presentation and diagnosis. The interviewee is a visualization expert and we employ, as a proof-of-concept, the unfolding of the cerebellum. The mesh of the cerebellum consists of 23,882 triangles and was obtained from the publicly accessible BodyParts3D database. With this usage scenario, we intend to show the ability of the *VisualFlatter* to help experts in identifying the a-priori-known distortion effects, such as strong area distortions of a Mercator projection **(T1)**. Also, we want to enable the user to perform a detailed analysis of

the distortions induced at every step of the projection pipeline (inflation and flattening) **(T2)** and to select alternatives that provide minimal distortion in the outcome **(T3)**.

The analysis of the projection of the cerebellum starts by comparing an angle-preserving sphere mapping algorithm with the area-preserving Lambert mapping. Larger changes of the area and low changes in angle are expected during the sphere mapping step. Also, low changes in area and larger changes in angle are expected during the cartographic unfolding. It is also known that the poles

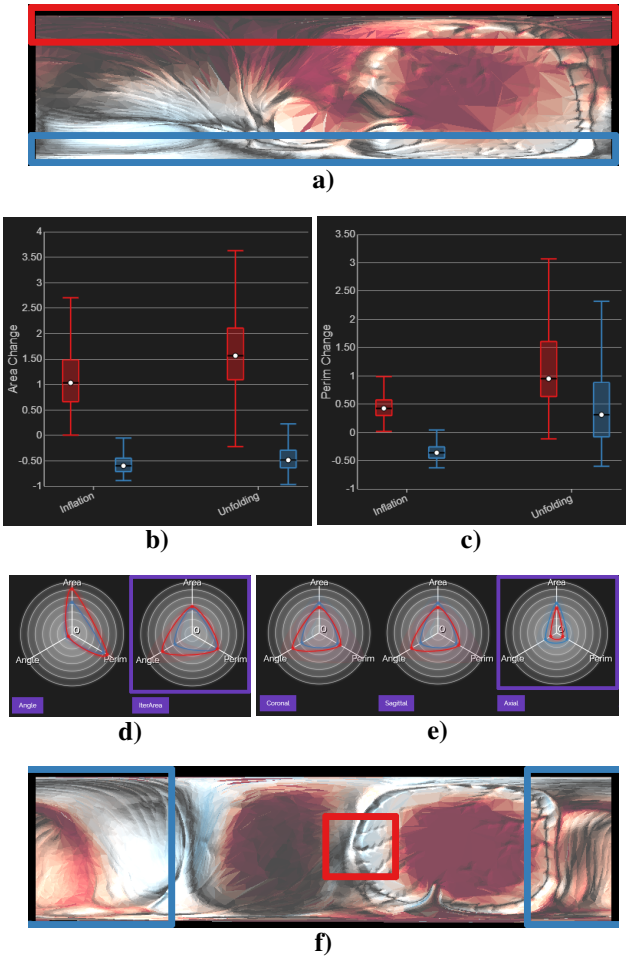

Figure 8: *The workflow of the cerebellum usage scenario. The goal is to minimally distort the region around the north and south pole, marked with the red and blue boxes (a). Inspection of the two boxplots (b) and (c) shows that the area is distorted during inflation, while the perimeter is largely distorted in the flattening step. The first problem can be solved by comparing the two possible sphere mapping algorithms using (d), and selecting the iterative area preserving one. The second problem seems to be the result of the selected cutting plane (e), where axial cutting distorts our selected regions the least in terms of perimeter. The final result (f) suffers less from overall area distortion, while being able to preserve the selected regions.*

suffer more from distortions. We can immediately notice, based on the area distortion coloring, that the concave part at the top of Figure 8-(a, red) got distorted, while the more convex parts shrank. This can be explained by the fact that the sphere mapping algorithm enlarges regions closer to the center **(T1)**. Looking at the angle and the perimeter distortion, we can see that both the north (red) and south (blue) pole suffer from larger distortions, which is a known property of many map projections. Exploring the box plots of the distortion measures for each transformation step of Figure 8-(b,c), we notice large area distortion in the first step through the angle preserving sphere mapping and the area-preserving second step, which tends to distort the angles and perimeters at the poles **(T2)**. For task **(T3)**, we assume that the currently selected regions (Figure 8-(a, red and blue)) are for some reason more important to be preserved. To improve the outcome of the projection, a representation where both areas display as low as possible distortions is sought. By comparing the two different sphere mapping algorithms, we see that the angle-preserving largely distorts the area of the red region, while the area-preserving transforms both regions comparably (Figure 8-(d)). So, the latter is selected. Also, the cutting plane has a huge influence on the local distortions, as it defines which regions are closer to the stronger distorted poles. The radar plot helps to determine that the axial cutting plane leads to least distortions (Figure 8-(e)).

The interviewed visualization expert of this usage scenario commented that the *VisualFlatter* is very suitable for the initial exploration of structures and their deformations. For example, it is easy to determine if a certain projection, inflation method or cutting is appropriate for a specific structure. The expert also commented that he would have appreciated to have such a tool, while creating his projection methods, as it would have helped him to analyze whether the result is trustable after the flattening and the extent of preservation of the initial structures. A direction for potential improvement, in his opinion, is to incorporate more scalar information and to add more unfolding methods, also more complex ones.

Scenario 2: Bladder radiation maps. During radiotherapy treatment of prostate cancer, the surrounding tissues, such as the bladder, might be also affected by radiation. This is not a desired effect and can have severe impacts on patients. Medical physicists need to precisely assess the extent of the affected bladder tissue, which is often done in projected 2D maps of the bladder surface [PBC*16, RCMA*18]. The bladder surface is inflated to a sphere, then projected on a 2D plane and the planned irradiated dose is shown on these so-called surface maps. In this scenario, we explore such a bladder-dose surface map together with a medical physicist. The unfolded mesh of the bladder consists of 5,460 triangles and was provided by the interviewee. Our aim is to explore the distortion introduced by the projection on the bladder surface **(T1)**, and build a projection setup where minimal distortions are introduced to the parts of the bladder that are more adjacent to the treated prostate **(T2, T3)**.

We create within the *VisualFlatter* a bladder-dose surface map, under the constraint that the regions close to the prostate (subject to higher radiation doses) should suffer from minimal distortions. Due to the lack of local geometric structures on the surface of the bladder, area preservation is favored over angle preservation. Adding

the radiation dose per triangle as an additional variable in the PCP allows the selection of regions with high irradiation in the 3D and 2D views, as shown in Figure 9-(a). In (b), the bladder surface is split into regions based on levels of irradiation. We need to determine if the high radiation areas are distorted more than other parts, to compare different cutting planes and select the one with the lowest distortion for these areas. To this end, the radar plots of Figure 9-(c) are employed. The manual arbitrary cutting plane (on the right), which was interactively selected by the user as the plane parallel to the interface between prostate and bladder, grants least distortion for the high radiation regions (Figure 9-(d)).

The interviewed medical physicist commented that the functionality of adding the radiation dose as an additional analysis parameter, defining a threshold for it and prioritizing the respective areas is very useful. He mentioned that such tools would be highly appreciated by people working on surface maps, where the main criticism against their use is the introduction of distortion and, subsequently, mistrust in the representation. He appreciated that the *VisualFlatter* enables to evaluate and optimize for the distortion in the high dose regions and he believes that it could be useful for prospect toxicity studies. As feedback, he proposed to extend the mapping to cylindrical projections for other organs, such as the rectum.

Scenario 3: Molecular surface maps. This usage scenario is different from the previous. Instead of analyzing medical structures, we show how it it can be applied to molecular biology, such as the data employed by Krone et al. [KFS*17]. The data included the original mesh and the spherical mapping step, and consisted of 17,722 triangles. It was provided by the interviewee. Besides the vertex positions, the data also contained labels for the different regions on the surface of the molecules. Our aim is to explore the distortion introduced by the different steps of the projection on the molecular surface **(T1, T2)**, and aid decision making when designing a new projection method **(T3)**.

Adding the labels of the molecular regions as an additional variable in the PCPs allows the selection and monitoring during the projection process. Using our approach, we see that the spherical mapping preserves the area distortion of nearly the entire mesh. Only a small part at the top and small triangles spread over the mesh suffer from severe area distortions. We filter only three individual active regions (specific amino-acid locations) based on their label (Figure 10-(a,b)). Two of these regions (yellow, blue) are very well preserved, while the third one (red) seems to be distorted due to its proximity to the extruded top part.

The interviewed visualization expert was interested in the projection methods and the inflation methods we use (Mercator and Lambert – conformal and iterative area). Most of the distortion is introduced during the inflation step and he appreciated the interactive cutting of the sphere, which would enable him to cut over the so-called active site of molecules. He liked the region selection when drawing over the 3D molecule and the possibility of being able to investigate the 3D mesh too. He commented that the *VisualFlatter* is useful for insight on the location of uncertainties.

Scenario 4: Segmentation error analysis. Automatic segmentation methods are often preferred for the delineation of organs, but due to high anatomical variability [RBGR18], they do not always perform optimally. The exploration of segmentation errors can also be done in a projected view of the resulting meshes. The provided data of this project consist of an average shape model of the prostate and its surrounding organs, which is the starting point for a specific Statistical Shape Modeling algorithm [SBV*13], and the adapted resulting meshes for three individual patients. Each mesh consists of 11,530 triangles, and each triangle is accompanied by an error measure, indicating its deviation from the ground truth. Our aim is to explore the distortion introduced during the optimization of

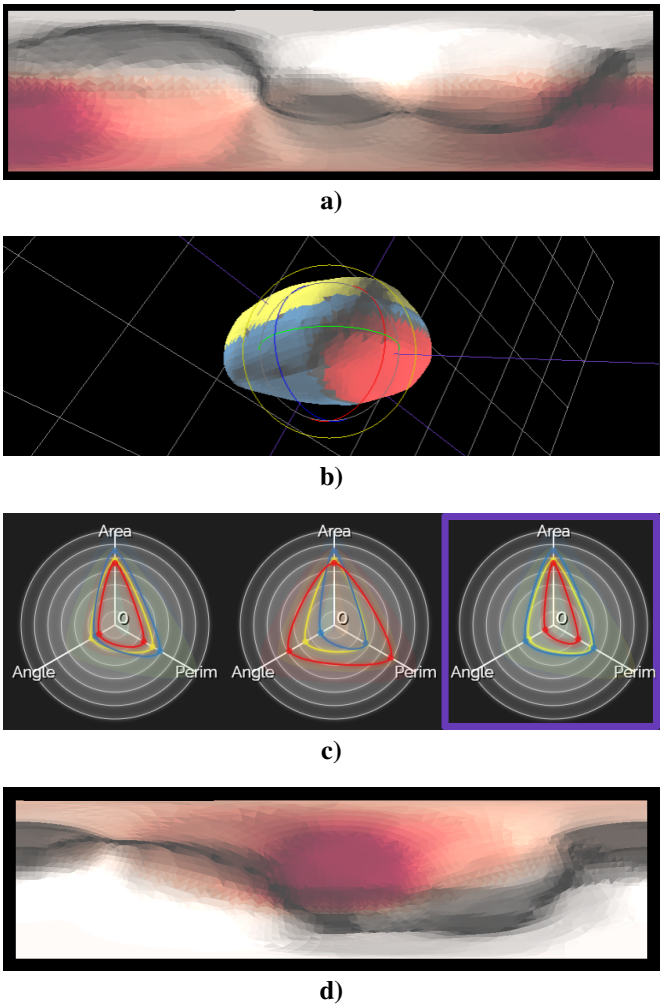

Figure 9: *The workflow of the bladder radiation maps usage scenario. The radiation dose can be overlayed on the 2D view of the bladder and used as an additional feature for the analysis (a). In the 3D view of a bladder, three regions are selected (b), accompanied by three radar plots (c) for individual cutting planes (coronal, axial, manual arbitrary). The red region was selected using the parallel coordinate plot and contains areas with high radiation. The goal is to minimally distort the red region, as it is the riskiest. The radar plot on the right displays the least distortion for the red region, which can be achieved with the manual cutting plane. The unfolding obtained with this plane, color-coded according to the amount of radiation, is shown in (d).*

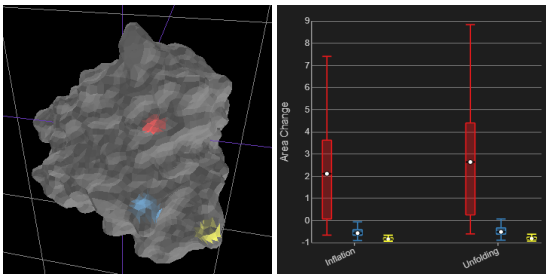

Figure 10: *The workflow of the molecular usage scenario. We show the selection of three regions that correspond to the same type of molecular structure (a,b). The red region shows the highest distortion, while the other two are preserved better. Most of the distortion is introduced during the spherical mapping in the first step.*

the SSM algorithm on the different organs **(T1)**, and explore comparatively the three provided patients to identify where minimal distortions are introduced **(T2, T3)**.

By setting the average model as the initial mesh, we can analyze the deformation during optimization for each patient. The provided error measures and additional labels identifying the individual organs can be used for defining selections of regions-of-interest. This allows us to identify the organs where segmentation errors are large, such as the bladder and the rectum. Instead of comparing several projection steps, we can use our box-plot to compare segmentations of individual patients. This allows us, for example, to identify patients that outstand in terms of distortion measures or segmentation errors, and detect whether there is a correlation among them. For example, errors are lower overall for patient 2, as shown in Figure 11-(c). For patient 1 shown in (b), the rectum has higher errors, but lower distortions than the other organs. The bladder has been well-segmented and also not very distorted. The prostate and the seminal vesicles display a lower segmentation error, but quite high distortions, which is consistent with the high anatomical variability of these organs. Patient 3 (d) shows the opposite behavior. This is also confirmed by the box plots view in Figure 11-(e).

The interviewed visualization expert of this usage scenario commented that the *VisualFlatter* can be used as an initial basis for many applications, where projections are used as a means to facilitate comparison of meshes. The tool is easy to use and easy to understand, while the employed plots are familiar to visualization experts, and potentially also to domain experts. The box plots are useful when comparing different patients, like in this scenario, but for the exploration of the evolution of errors, a more versatile representation could be used.

5.2. Generic evaluation

We further abstract our tool from a specific biomedical application and apply it to a broader case of mesh projection. The purpose was to make it accessible and understandable for a wider public, which – still – is knowledgeable about projections. We conducted an evaluation with 13 visualization experts, out of which 11 had worked

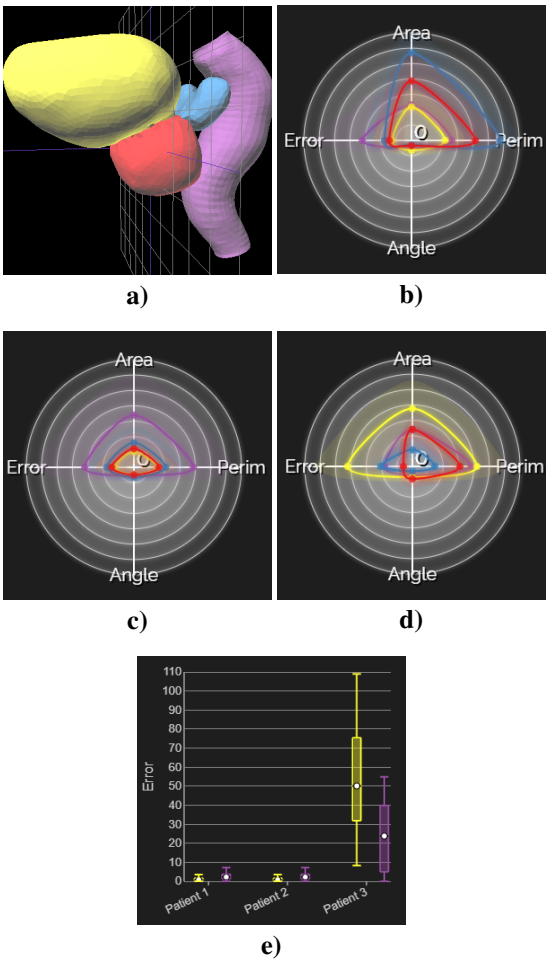

Figure 11: *The workflow of the segmentation error analysis usage scenario. The four individual organs represent separate regions in the initialization model (a). We extend the radar plots (b-d), using an additional fourth axis for the provided error measure of the segmentation. Each radar plot corresponds to a different patient. We see that errors are lower overall for patient 2 (c). For example, for patient 1 the distortion is higher for the seminal vesicles, but the error is still small (b), while the opposite happens for the other two patients (c-d). The box plots can also be used to explore the segmentation error for three patients, for the bladder (yellow) and rectum (purple) (e).*

with some projection method before. We provided them a scenario of mesh projection, for which the Stanford bunny mesh was used. Then, we asked them questions (with a unique correct answer) that were related to each one of the three tasks that can be completed with the *VisualFlatter* **(T1-T3)**. Our goal was to see whether these tasks could be performed with the selected encodings and to solicit their feedback with respect to the design choices of our tool.

For the exploration and analysis of the distortions **(T1)**, 11 were able to correctly identify areas with a specific high distortion measure (area distortion) and 11 were able to correctly identify areas with overall low distortions (area, angle and perimeter), in the radar

plots. All 13 were able to correctly interpret the deviations depicted by the areas in the radar plots, also, for one individual distortion measure and for the overall distortion. At this point, most of them (12) commented that the radar plots are useful for comparing regions and their respective distortions, and also understandable both in terms of average distortion and deviation (12). One person commented that "*It would be nice to see also a distribution of the properties (e.g., as small histogram on each axis)*". For the exploration and analysis of the progression of distortions over the projection process **(T2)**, only 7 were able to correctly identify which step introduces more distortion to the process. A potential reason for that could be that the participants misinterpreted the representation, which shows the errors cumulatively. In a different example, all of them were able to identify which step of the pipeline can be improved to reduce distortions. Also, all of them could correctly determine which of the distortion measures are affected during the different steps. The boxplots of were considered useful by 12 people, but less (8) found them easily understandable. As one person mentioned: "*combining two steps into one diagram makes it harder to distinguish. Furthermore, the attribute (perim, angle, area) was not highlighted enough, so it took me quite a long time to figure out which boxplot corresponds to which attribute*". Finally, for the exploration and informed selection of appropriate projection setups **(T3)**, in all examined cases, all participants were able to identify the setups that are able to minimize distortions. Here, one participant noted that "*without the radar plots I would not have been able to judge which projection is more distorting*, while another one commented that "*comparing the area in the unfolded mesh is difficult for humans if the angle and perimeter are not preserved. I think this might be a benefit of your technique*".

6. Conclusion and future work

We presented the *VisualFlatter*, a visual tool that allows experts to analyze in a structured way the distortions introduced on 3D meshes, across projection processes. We presented a workflow that facilitates the global analysis of distortions. In addition to that, the user can split the mesh into regions-of-interest, which can be analyzed individually, to understand local distortions. We provide a way for visualization experts to compare different parametric setups of projection processes, to support decision making in the design of such methods. We showed the applicability of this tool for several use-cases, such as the unfolding of organ meshes, the generation of molecular surface meshes to 2D maps, or the segmentation analysis of pelvic organ projections.

There are several possible directions for future work, starting from the extensibility of the approach from mere 3D mesh exploration and analysis to entire volumetric datasets. This will require adaptations to the proposed approach, in order to include an extended set of distortion measures, such as neighborhood displacement, or surface feature preservation. By adding more distortion measures, the scalability of the employed visualizations might pose an issue, and other visual representations would be required. Another interesting topic would be a more in-depth exploration of the projection process. This would require to include a higher number of steps for the follow-up studies of the distortion evolution through the entire process, to investigate the propagation, accumulation and trade-off between distortions. All in all, our proposed *VisualFlatter* is a promising basis, which allows experts to conduct an in-depth analysis of their projection algorithms, aiding them to improve their methods and results, in the future.

7. Acknowledgements

This paper was partly written in collaboration with the VRVis Competence Center. VRVis is funded by BMVIT, BMWFW, Styria, SFG and Vienna Business Agency in the scope of COMET - Competence Centers for Excellent Technologies (854174), managed by FFG. The authors would like to thank Karsten Schatz (University of Stuttgart, Germany), Haichao Miao (TU Wien, Austria) and Oscar Casares-Magaz (Aarhus University Hospital, Denmark) for their contribution to the evaluation and for the fruitful discussions.

References

[AH11] ANGELELLI P., HAUSER H.: Straightening tubular flow for side-by-side visualization. *IEEE Transactions on Visualization and Computer Graphics 17*, 12 (2011), 2063–2070. 2

[AMB*13] AUZINGER T., MISTELBAUER G., BACLIJA I., SCHERNTHANER R., KÖCHL A., WIMMER M., GRÖLLER M. E., BRUCKNER S.: Vessel visualization using curved surface reformation. *IEEE Transactions on Visualization and Computer Graphics 19*, 12 (2013), 2858–2867. 2

[BPS10] BALASUBRAMANIAN M., POLIMENI J. R., SCHWARTZ E. L.: Near-isometric flattening of brain surfaces. *NeuroImage 51*, 2 (2010), 694–703. 2

[CCKT83] CHAMBERS J., CLEVELAND W., KLEINER B., TUKEY P.: *Graphical Methods for Data Analysis*. Wadsworth ed., 1983. 5

[CLL15] CHOI P. T., LAM K. C., LUI L. M.: Flash: Fast landmark aligned spherical harmonic parameterization for genus-0 closed brain surfaces. *SIAM Journal on Imaging Sciences 8*, 1 (2015), 67–94. 3, 6

[CPS13] CRANE K., PINKALL U., SCHRÖDER P.: Robust fairing via conformal curvature flow. *ACM Transactions on Graphics (TOG) 32*, 4 (2013), 61. 4

[FH05] FLOATER M. S., HORMANN K.: Surface parameterization: a tutorial and survey. In *Advances in Mltiresolution for Geometric Modelling*. Springer, 2005, pp. 157–186. 4

[HATK00] HAKER S., ANGENENT S., TANNENBAUM A., KIKINIS R.: Non-distorting flattening for virtual colonoscopy. In *International Conference on Medical Image Computing and Computer-Assisted Intervention* (2000), Springer, pp. 358–366. 2

[HB03] HARROWER M., BREWER C. A.: Colorbrewer. org: an online tool for selecting colour schemes for maps. *The Cartographic Journal 40*, 1 (2003), 27–37. 4, 5

[HK14] HASS J., KOEHL P.: How round is a protein? exploring protein structures for globularity using conformal mapping. *Frontiers in molecular biosciences 1* (2014), 26. 2

[HN98] HINTZE J. L., NELSON R. D.: Violin plots: a box plot-density trace synergism. *The American Statistician 52*, 2 (1998), 181–184. 5

[Ins85] INSELBERG A.: The plane with parallel coordinates. *The visual computer 1*, 2 (1985), 69–91. 4

[KBH*10] KOK P., BAIKER M., HENDRIKS E. A., POST F. H., DIJKSTRA J., LOWIK C. W., LELIEVELDT B. P., BOTHA C. P.: Articulated planar reformation for change visualization in small animal imaging. *IEEE Transactions on Visualization and Computer Graphics 16*, 6 (2010), 1396–1404. 2

[Kei02] KEIM D. A.: Information visualization and visual data mining. *IEEE Transactions on Visualization and Computer Graphics 8*, 1 (2002), 1–8. 5

[KFS*17] KRONE M., FRIESS F., SCHARNOWSKI K., REINA G., FADEMRECHT S., KULSCHEWSKI T., PLEISS J., ERTL T.: Molecular surface maps. *IEEE Transactions on Visualization and Computer Graphics 23*, 1 (2017), 701–710. 2, 6, 8

[KFW*02] KANITSAR A., FLEISCHMANN D., WEGENKITTL R., FELKEL P., GRÖLLER M. E.: CPR: curved planar reformation. In *Proceedings of the Conference on Visualization* (2002), IEEE Computer Society, pp. 37–44. 2

[KLR*13] KLEMM P., LAWONN K., RAK M., PREIM B., TÖNNIES K. D., HEGENSCHEID K., VÖLZKE H., OELTZE S.: Visualization and analysis of lumbar spine canal variability in cohort study data. In *Proceedings of International Symposium on Vision, Modeling and Visualization (VMV)* (2013), pp. 121–128. 2

[KMM*18] KREISER J., MEUSCHKE M., MISTELBAUER G., PREIM B., ROPINSKI T.: A Survey of Flattening-Based Medical Visualization Techniques. *Computer Graphics Forum* (2018). 1, 2

[KST*14] KRETSCHMER J., SOZA G., TIETJEN C., SUEHLING M., PREIM B., STAMMINGER M.: ADR-Anatomy-Driven Reformation. *IEEE Transactions on Visualization and Computer Graphics 20*, 12 (2014), 2496–2505. 2

[KSZ14] KHOSRAVI H., SOLTANIAN-ZADEH H.: Multi-surface quasi-isometric flattening of the cortex. In *IEEE 11th International Symposium on Biomedical Imaging (ISBI)* (2014), IEEE, pp. 1226–1229. 2

[Mis13] MISTELBAUER G.: Smart interactive vessel visualization in radiology. *PhD Thesis, TU Wien, Austria* (2013). 2

[MMK*17] MIAO H., MISTELBAUER G., KARIMOV A., ALANSARY A., DAVIDSON A., LLOYD D. F., DAMODARAM M., STORY L., HUTTER J., HAJNAL J. V., ET AL.: Placenta maps: In utero placental health assessment of the human fetus. *IEEE Transactions on Visualization and Computer Graphics 23*, 6 (2017), 1612–1623. 2, 6

[NSZ*17] NADEEM S., SU Z., ZENG W., KAUFMAN A. E., GU X.: Spherical parameterization balancing angle and area distortions. *IEEE Transactions on Visualization and Computer Graphics 23*, 6 (2017), 1663–1676. 4

[PBC*16] PALORINI F., BOTTI A., CARILLO V., GIANOLINI S., IMPROTA I., IOTTI C., RANCATI T., COZZARINI C., FIORINO C.: Bladder dose–surface maps and urinary toxicity: Robustness with respect to motion in assessing local dose effects. *Physica Medica: European Journal of Medical Physics 32*, 3 (2016), 506–511. 6, 7

[PH03] PRAUN E., HOPPE H.: Spherical parametrization and remeshing. In *ACM Transactions on Graphics (TOG)* (2003), vol. 22, ACM, pp. 340–349. 2

[PS09] POSTARNAKEVICH N., SINGH R.: Global-to-local representation and visualization of molecular surfaces using deformable models. In *Proceedings of the 2009 ACM symposium on Applied Computing* (2009), ACM, pp. 782–787. 2

[RBGR18] REITER O., BREEUWER M., GRÖLLER M. E., RAIDOU R.: Comparative visual analysis of pelvic organ segmentations. *Computer Graphics Forum* (2018), 037–041. 3, 8

[RCMA*18] RAIDOU R., CASARES-MAGAZ O., AMIRKHANOV A., MOISEENKO V., MUREN L. P., EINCK J. P., VILANOVA A., GRÖLLER M. E.: Bladder Runner: Visual Analytics for the Exploration of RT-Induced Bladder Toxicity in a Cohort Study. *Computer Graphics Forum 37*, 3 (2018), 205–216. 2, 7

[RMB*16] RAIDOU R. G., MARCELIS F. J., BREEUWER M., GRÖLLER E., VILANOVA A., VAN DE WETERING H. M.: Visual analytics for the exploration and assessment of segmentation errors. In *Proceedings of Eurographics Workshop on Visual Computing for Biology and Medicine (EG VCBM)* (2016), pp. 193–202. 3, 6

[RS07] RAHI S. J., SHARP K.: Mapping complicated surfaces onto a sphere. *International Journal of Computational Geometry & Applications 17*, 04 (2007), 305–329. 2

[Sar06] SAROUL L.: Surface extraction and flattening for anatomical visualization. *PhD Thesis, Ecole Polytechnique Federale De Lausanne, Switzerland* (2006). 2

[SBV*13] SCHADEWALDT N., BYSTROV D., VIK T., SCHULZ H., PETERS J., FRANZ A., BUERGER C., BZDUSEK K.: Robust initialization of multi-organ shape models. In *MICCAI Challenge Workshop on Segmentation: Algorithms, Theory and Applications* (2013), vol. 1, p. 3. 8

[SMS09] SILVA S., MADEIRA J., SANTOS B. S.: PolyMeCo: An integrated environment for polygonal mesh analysis and comparison. *Computers & Graphics 33*, 2 (2009), 181–191. 3

[Sny97] SNYDER J. P.: *Flattening the earth: two thousand years of map projections*. University of Chicago Press, 1997. 1, 2, 3, 4

[SPA*14] SCHMIDT J., PREINER R., AUZINGER T., WIMMER M., GRÖLLER M. E., BRUCKNER S.: Ymca: Your mesh comparison application. In *IEEE Conference on Visual Analytics Science and Technology (VAST)* (2014), IEEE, pp. 153–162. 3

[TBB*08] TERMEER M., BESCÓS J. O., BREEUWER M., VILANOVA A., GERRITSEN F., GRÖLLER M. E., NAGEL E.: Visualization of myocardial perfusion derived from coronary anatomy. *IEEE Transactions on Visualization and Computer Graphics 14*, 6 (2008), 1595–1602. 2

[VBWKG01] VILANOVA BARTROLÍ A., WEGENKITTL R., KÖNIG A., GRÖLLER E.: Nonlinear virtual colon unfolding. In *Proceedings of the Conference on Visualization* (2001), IEEE Computer Society, pp. 411–420. 2

[VW08] VAN WIJK J. J.: Unfolding the earth: myriahedral projections. *The Cartographic Journal 45*, 1 (2008), 32–42. 1

[ZHT05] ZHU L., HAKER S., TANNENBAUM A.: Flattening maps for the visualization of multibranched vessels. *IEEE Transactions on Medical Imaging 24*, 2 (2005), 191–198. 2